BMC Plant Biology

RESEARCH

Open Access

Multi-omics analysis reveals key regulatory defense pathways in *Ruppia sinensis* in response to water salinity fluctuations

Yang Zou[1] and Xinwei Xu[1*]

Abstract

Seagrasses maintain cellular water balance by regulating ion concentrations and accumulating organic osmolytes, enabling them to survive in the fluctuating salinity of intertidal environments. However, the molecular mechanisms underlying seagrass responses to salinity changes remain relatively understudied. To address this, we conducted a multi-omics analysis of *Ruppia sinensis* under low, moderate, and high salinity conditions to uncover the mechanisms behind its adaptation to salinity fluctuations. Our research revealed that the transition from low to high salinity significantly altered the physiological characteristics of *R. sinensis*. Simultaneously, the species enhanced its ability to cope with and adapt to salinity fluctuations by increasing antioxidant enzyme activity. Integration of multi-omics data further indicated that under high salinity conditions, *R. sinensis* synthesizes more flavonoids to bolster its adaptive capacity. Additionally, the phenylpropanoid metabolic pathway appears to play a crucial role in the response of *R. sinensis* to changes in water salinity.

Keywords Transcriptome, Proteome, Metabolome, *Ruppia Sinensis*, Phenylpropanoid pathway, Salt stress

Background

The response of plants to salt stress has been one of the hottest research topics in botany and ecology. Salinity stress inhibits plant growth and development through various mechanisms [27]. High salinity induces osmotic stress, reducing external water potential, which makes it difficult for plants to absorb water and triggers physiological responses such as a rapid decline in turgor pressure in root and stem cells [19, 46]. To cope with this, plants may absorb inorganic ions to restore turgor pressure, but this often results in reduced growth rates [59]. Additionally, salt stress can lead to stomatal closure, limiting carbon dioxide assimilation and causing the excessive accumulation of Na^+ and Cl^- ions within cells, which disrupts normal metabolic functions [13]. To alleviate the oxidative stress associated with salinity, plants activate a complex antioxidant defense system that relies on non-enzymatic antioxidants (such as ascorbate, glutathione, and tocopherol) and enzymatic antioxidants (such as catalase, superoxide dismutase, ascorbate peroxidase, and glutathione reductase) to scavenge excess reactive oxygen species (ROS) and maintain redox homeostasis [62]; Kerchey et al., [35]; Mishra et al., [45]. The phenylpropanoid pathway plays a vital role in this process, synthesizing a range of compounds such as flavonoids, lignin, and phenolic compounds, which not only enhance antioxidant capacity but also strengthen cellular structures [51, 54, 68, 72]. As key products of this pathway, flavonoids can directly scavenge ROS, mitigating oxidative damage, and contribute to osmotic regulation, helping plants maintain cellular homeostasis [28, 60]. Meanwhile, lignin and phenolic compounds fortify the cell wall, reducing structural damage caused by salt stress [16, 39].

*Correspondence:
Xinwei Xu
xuxw@whu.edu.cn
[1] National Field Station of Freshwater Ecosystem of Liangzi Lake, College of Life Sciences, Wuhan University, Wuhan 430072, China

Through these mechanisms, plants can adapt to salinity stress, enhancing their overall tolerance and minimizing the negative impacts on growth and development. However, current research on salt tolerance mechanisms has mainly focused on terrestrial plants or emergent species [20, 31, 40, 54, 66], and there is still a relatively limited understanding of the molecular mechanisms by which submerged plants respond to salt stress.

Understanding how seagrasses adapt to environmental changes is crucial for the conservation and management of marine ecosystems. Fluctuations in water salinity profoundly affect the physiological and biochemical processes of seagrasses and are one of the key factors leading to their decline [65]. In response to salt stress, seagrasses have developed a range of adaptive strategies, including changes in signaling pathways, reactive oxygen species (ROS) accumulation, activation of antioxidant systems, maintenance of redox balance, and osmotic regulation [30]. Compared to their freshwater relatives, seagrasses exhibit a notable tolerance to varying salinity levels, which is a critical ecological factor influencing their survival, growth, and distribution [9]. Salinity fluctuations can disrupt the osmotic balance of seagrass cells, impairing their physiological and biochemical functions and ultimately affecting their survival [46]. For instance, high salinity conditions can reduce the levels of non-structural carbohydrates, glutamate synthase activity, and growth potential in seagrasses [18]. Additionally, an increase in salt-tolerant algae under high salinity conditions can have negative effects on seagrass ecosystems [43].

Ruppia sinensis, a species of seagrasses widely distributed in coastal and inland regions of China, thrives in saline and brackish environments and shows remarkable adaptability to varying salinity levels [26]. It typically inhabits coastal lagoons, estuaries, abandoned salt ponds, and inland saline waters, where it serves as a crucial primary producer, playing an essential role in maintaining ecological balance. Compared to other submerged angiosperms, *Ruppia* exhibits greater flexibility in its salinity tolerance range [10]. For instance, in the shallow lakes of Western Australia, *Ruppia* can survive in waters with total dissolved solids (TDS) ranging from 3.7 to 78.3 parts per thousand (PPT), and its seeds remain viable even when TDS levels reach 81.7 to 142.0 PPT [23]. Under controlled conditions, *R. sinensis* can grow in water with salinity levels ranging from 0 to 35 PPT, and seed germination studies indicate that significant inhibition only occurs in highly saline conditions (40 to 50 PPT) [25]. Given its resilience to high and fluctuating salinity, *R. sinensis* represents an ideal model for investigating the genetic mechanisms underlying salinity adaptation in seagrasses. In recent years, transcriptomics, proteomics, and metabolomics have emerged as powerful tools for unraveling complex biological responses, particularly in studies examining plant responses to abiotic stress [56]. The integration of these three omics approaches offers a systematic avenue to explore the mechanisms of salinity adaptation in seagrasses. However, in-depth studies on the salinity tolerance and response mechanisms of seagrasses remain scarce. This study aimed to uncover the molecular mechanisms of *R. sinensis* in response to salinity fluctuations by multi-omics analysis, making our knowledge of plant salt tolerance mechanisms more comprehensive.

Materials and methods

Plant material and salt treatment

Mature seeds of *R. sinensis* were collected from a pond with a salinity of 5 PPT in Yancheng, Jiangsu Province, China (33.83°N, 120.47°E). All collection activities were approved by local authorities and competent authorities. The mature seeds of *R. sinensis* were identified by Associated Prof. Wei Du, a plant taxonomist from Wuhan University. A voucher specimen was deposited in the Herbarium of Wuhan University, with voucher number WH164007. Sediments from the growth site were transported to the laboratory and mature seeds were separated by sediment filtration. The collected seeds were then stored in a high-salinity solution containing 45 PPT NaCl to inhibit germination. The experiment was conducted in a growth chamber under conditions of 16 h of light at 26 °C and 8 h of darkness at 18 °C. Temperature settings simulated the natural conditions of the location where *R. sinensis* was collected during its growing season in May. And light hours were two hours longer than the natural conditions to ensure rapid plant growth after germination. Initially, the seeds of *R. sinensis* underwent stratification at 0 °C for three days before being hydroponically cultured in a half-strength modified Hoagland nutrient solution with 5 PPT NaCl, which is the optimal salinity for the germination of *R. sinensis* seeds [25]. A total of 200 seeds were placed in each culture flask, with three replicate flasks prepared. After germination, the seedlings were cultivated under the same conditions for 15 days. The plants were then transferred to culture flasks with different salinities (0 PPT, 14 PPT, and 28 PPT). Each flask contained 50 plants to meet the sample quantity requirements for subsequent sequencing, and the plants were treated for 7 days (Fig. S1). Three biological replicates per treatment were used for transcriptomic and proteomic analyses, while six biological replicates per treatment were used for metabolomic analyses to ensure sufficient statistical power and robustness due to the complexity and variability of metabolic profiles. Finally, leaf tissues (excluding roots) were harvested for

physiological measurements, transcriptomic, proteomic, and metabolomic analyses.

Determination of physiological indexes

Following the method described by Lichtenthaler and Wellburn [41], the absorbance of chlorophyll extracted with 96% ethanol was measured at 470 nm using a spectrophotometer, and total chlorophyll content was calculated using the corresponding formula. Soluble protein content was determined using the Bradford method, with bovine serum albumin as the standard [11]. Malondialdehyde (MDA) content was assessed using the thiobarbituric acid (TBA) method as described by Chai et al. [14]. Specifically, MDA extraction solution was mixed with 0.67% TBA and heated at 100 °C for 30 min, followed by centrifugation at 15,000 r/min for 10 min at 4 °C. The absorbance of the supernatant was then measured at 600 nm. The concentrations of soluble protein and MDA were calculated using the respective formulas.

The activities of superoxide dismutase (SOD), peroxidase (POD), and catalase (CAT) were determined following the protocols outlined by Xu et al. [70]. SOD activity was measured by assessing the absorbance at 560 nm in a 3 mL reaction mixture containing 0.3 mL of 260 mM methionine, 0.3 mL of 750 μM NBT, 0.3 mL of 100 μM EDTA-Na2, 0.3 mL of 20 μM riboflavin, 1.8 mL of variable volume phosphate buffer, and the enzyme extract. POD activity was determined by measuring the change in absorbance at 470 nm after adding 1 mL of enzyme extract to a 3 mL reaction mixture (comprising 28 μL of guaiacol and 19 μL of hydrogen peroxide in a 50 mL mixture). CAT activity was determined by monitoring the change in absorbance at 240 nm after adding 500 μL of enzyme extract to a mixture containing 2 mL of phosphate buffer and 500 μL of H_2O_2. All physiological parameters were measured using fresh leaf samples, with each measurement repeated three times to ensure data accuracy.

Transcriptome analysis

We generated 9 cDNA libraries for RNA-seq analysis, with three biological replicates for each treatment condition. Transcriptome sequencing was carried out by Shanghai Majorbio Biopharm Technology Co., Ltd. The purity and integrity of the RNA samples were evaluated using a Nanophotometer spectrophotometer and an Agilent 2100 Bioanalyzer. The RNA libraries were then sequenced on the Illumina HiSeq platform. The raw sequencing data were processed using Fastp with default parameters [15] to remove low-quality reads and adapter sequences. The cleaned reads were then aligned to the reference genome (https://figshare.com/s/f76874c59c477e4df3e3) using HISAT2 [38] with the following parameters: --dta --phred64 --unstranded --new-summary -x index −1 read_r1 −2 read_r2 for paired-end reads. Gene expression levels were measured in FPKM (fragments per kilobase of transcript per million mapped reads) using HTSeq [52]. Differentially expressed genes (DEGs) were identified using DESeq [2] with the criteria of an absolute |log2 fold change| ≥ 1 and a false discovery rate (FDR) < 0.05. To obtain comprehensive annotation information, we used BLAST [8] (E-value cut-off of ≤1e-5) to align the RNA-seq derived genes (unigenes) against six public databases: GO (https://geneontology.org/), KEGG [34], EggNOG [32], NR (http://www.ncbi.nlm.nih.gov/), Swiss-Prot [7], and Pfam [5]. We assessed the correlation of gene expression levels across RNA-Seq samples based on Pearson correlation coefficients and performed principal component analysis (PCA) using MetaboAnalyst [50].

DIA-based proteomics analysis

Frozen leaf samples were lysed on ice using a protein extraction buffer (8 M urea with protease inhibitors), followed by sonication for 2 min and lysis for 30 min. The lysates were centrifuged at 12,000 g for 30 min at 4 °C to collect the protein supernatant. Protein concentration was determined using the BCA method with BSA standards, and protein quality was assessed by SDS-PAGE. For digestion, 100 μg of protein was treated with TCEP, alkylated with iodoacetamide, and precipitated using pre-cooled acetone at −20 °C. The precipitate was collected by centrifugation, dissolved in TEAB, and digested with trypsin at a 1:50 enzyme-to-protein ratio.

The resulting peptides were desalted, dried by vacuum centrifugation, and reconstituted in 0.1% TFA. Peptides were then fractionated using high-pH reverse-phase liquid chromatography, yielding 20 fractions that were concentrated and reconstituted for mass spectrometry analysis. In DDA mode, the top 20 most intense precursor ions were selected for tanDAM MS analysis. For DIA analysis, equal amounts of peptides were reconstituted, spiked with iRT peptides, and analyzed. The DIA data were processed using Spectronaut software [6], extracting peaks based on spectral libraries to identify and quantify proteins in the samples. To obtain annotation information for these proteins, we performed BLAST (E-value cut-off of ≤1e-5) alignment against six public databases: NR, SubCell-Location (http://www.csbio.sjtu.edu.cn/bioinf/Cell-PLoc-2/), GO, KEGG, Pfam, and EggNOG. PCA and clustering heat maps were performed using MetaboAnalyst.

UHPLC-MS/MS-based untargeted metabolomics analysis

To begin the process, 100 mg of leaf samples ground in liquid nitrogen was added to an Eppendorf tube,

followed by the addition of 500 µL of 80% methanol solution. The sample was thoroughly mixed using a vortex and then placed on ice for 5 min. After this, it was centrifuged at 15,000 g and 4 °C for 20 min. From the resulting supernatant, 400 µL was taken and diluted with mass spectrometry grade water (Merck, Germany) to adjust the methanol concentration to 53%. This diluted solution was centrifuged again under the same conditions to further purify the supernatant, which was then prepared for UHPLC-MS/MS analysis. Quality control (QC) samples were created by pooling equal volumes from each experimental sample, and a 53% methanol-water solution underwent the same pretreatment as the samples to serve as a blank control.

The UHPLC-MS/MS analysis was conducted using a Vanquish UHPLC system equipped with a Hypersil Gold column (100 mm × 2.1 mm, 1.9 µm) maintained at 40 °C. For the positive ion mode, the mobile phases were 0.1% formic acid (solvent A) and methanol (solvent B); for the negative ion mode, 5 mM ammonium acetate (pH 9.0, solvent A) and methanol (solvent B) were used. The flow rate was set at 0.2 mL/min, with a gradient elution profile of 98% solvent A from 0 to 1.5 min, 15% solvent A from 1.5 to 3 min, 0% solvent A from 3 to 10 min, and returning to 98% solvent A from 10 to 12 min. The mass spectrometry analysis was performed using a Q Exactive™ HF-X mass spectrometer, which was set to detect in both positive and negative ion modes across an m/z range of 100–1,500. The instrument settings included a spray voltage of 3.5 kv, a sheath gas flow rate of 35 psi, an auxiliary gas flow rate of 10 L/min, a capillary temperature of 320 °C, an S-lens RF level of 60, and an auxiliary gas heater temperature of 350 °C. Differential metabolites were annotated using the KEGG, HMDB [69], and LIPID [63] Maps database. PCA and clustering heat maps were performed using MetaboAnalyst.

Candidate gene validation via qRT-PCR

Quantitative reverse transcription PCR (RT-qPCR) was conducted on nine differentially expressed genes (DEGs) within the phenylpropanoid pathway to validate the results obtained from high-throughput sequencing. Total RNA was extracted using the hot borate method and subsequently reverse transcribed with the HiScript III LIPID All-in-one RT SuperMix. Gene expression levels were then quantitatively measured using 2× ChamQ SYBR qPCR Master Mix. The relative expression of each gene was determined using the $2^{-\Delta\Delta Ct}$ method, with *GAPDH* serving as the internal reference gene. The specific primers utilized for RT-qPCR are detailed in Table S1.

Statistical analysis

Statistical analyses were performed using IBM SPSS Statistics, and graphical representations were created using GraphPad Prism [61]. Paired data comparisons were evaluated using Student's t-tests. Each experiment included at least three biological replicates, and error bars in the graphs represent the standard error (SE) of the mean. Bioinformatics analyses and data visualization were conducted using the Majorbio Cloud platform (https://www.majorbio.com/) and OmicShare tools (https://www.chiplot.online/). The DEGs, DAPs, and DAMs were annotated with Encyclopedia of Genes and Genomes (KEGG) (http://www.genome.ad.jp/kegg/) categories using the ClusterProfiler [73]. The significance of enrichment was defined as a P-value < 0.05 and FDR < 1.

Results

Physiological changes in *R. sinensis* in response to salt stress

After 7 days of exposure to three different salinity levels (0 PPT, 14 PPT, and 28 PPT), the physiological characteristics of *R. sinensis* showed significant changes. These changes included variations in catalase (CAT), peroxidase (POD), superoxide dismutase (SOD), malondialdehyde (MDA), soluble protein (SP), and total chlorophyll (Chl) levels (Fig. 1). The results indicated that *R. sinensis* enhances its ability to adapt to and resist fluctuations in water salinity by increasing its antioxidant enzyme activity. Salt stress generally leads to elevated levels of reactive oxygen species (ROS), with CAT, POD, and SOD activities being lowest at 0 PPT, increasing at 14 PPT, and reaching their highest levels at 28 PPT (Fig. 1). As key antioxidant enzymes, the increased activities of CAT, POD, and SOD help protect cells from oxidative damage. MDA and SP contents also increased with increasing salinity, following a similar trend. In contrast, Chl content decreased with increasing salinity.

Differentially expressed genes (DEGs) identification and functional annotation

Through RNA-seq sequencing, we obtained over 716 million raw reads, with an average of 79.62 million reads per sample. After rigorous quality control, 704 million clean reads were retained, of which 87.2% were uniquely mapped reads. Detailed information on the RNA-seq data, including the number of reads, Q30 values, data quality, and mapping ratios, was provided in Table S2. Based on these data, 44,200 expressed genes were identified, and the expression levels of all genes were quantified using FPKM values. The distribution of gene expression across all samples (Fig. S4) showed good reproducibility and reliability and consistent expression trends within

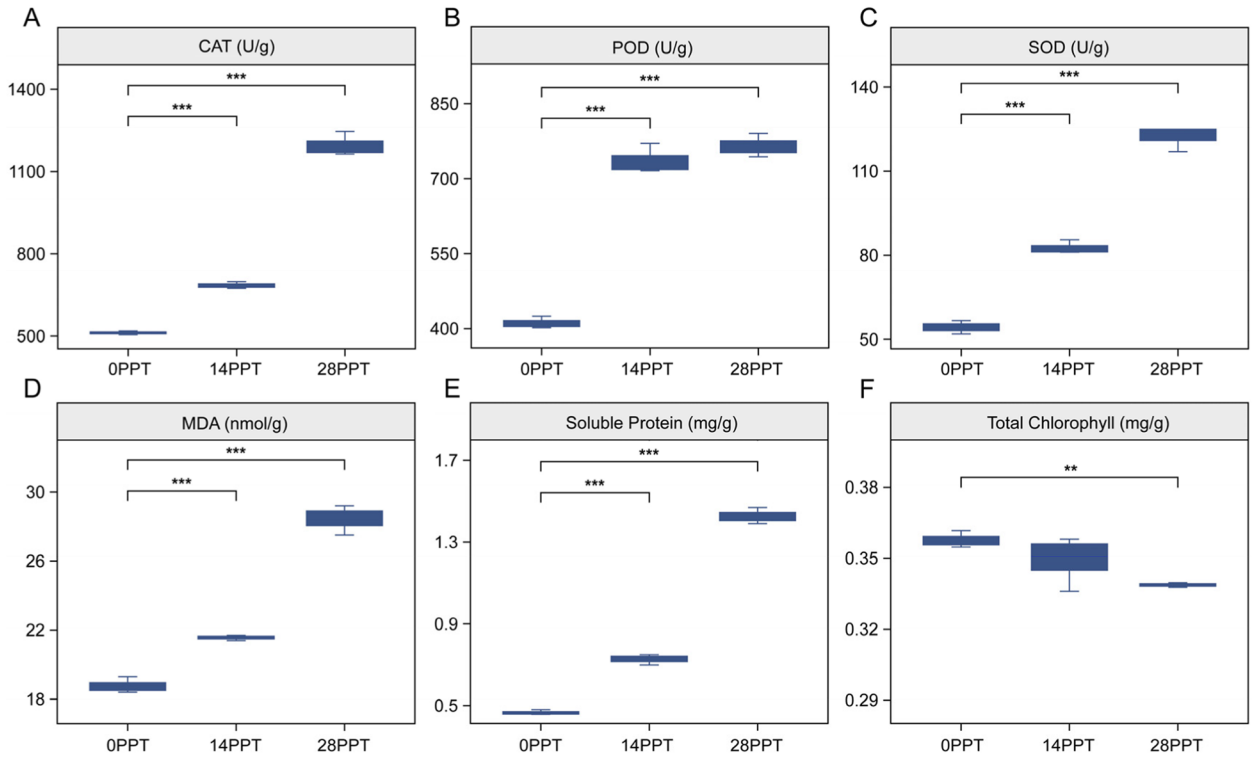

Fig. 1 Physiological changes in the leaves of *Ruppia sinensis* caused by salinity fluctuations. (**A**) Catalase, CAT. (**B**) Peroxidase, POD. (**C**) Superoxide dismutase, SOD. (**D**) Malondialdehyde, MDA. (**E**) Soluble protein, SP. (**F**) Total Chlorophyll. All data are presented as the mean ± standard deviation from three replicates. *** indicates $p < 0.01$, ** indicates $p < 0.05$

samples of the same treatment group. Annotation results showed that 35,502 unigenes were annotated in the NR database, representing 91.08% of the total, the highest proportion among all databases. This was followed by EggNOG (33,008 genes, 83.26%), GO (30,914 genes, 79.12%), Pfam (30,537 genes, 76.84%), Swiss-Prot (28,698 genes, 71.60%), and KEGG (15,135 genes, 36.37%) (Fig. S3).

To identify DEGs with significant changes, we set the screening criteria to $|\log FC| \geq 1$ and $p < 0.05$ and conducted a statistical analysis of the expression of these DEGs (Fig. 2A and B). In the 14 PPT_vs_0 PPT group, 2,908 DEGs were identified, with 1,625 upregulated and 1,283 downregulated. This indicates significant changes in gene expression under these salinity conditions in *R. sinensis*. In the 28 PPT_vs_14 PPT group, the number of DEGs increased to 6,623, with 2,914 upregulated and 3,709 downregulated (Fig. 2A and B), suggesting that gene expression changes become more pronounced with increasing salinity. Additionally, we performed a KEGG enrichment analysis on the DEGs across the comparison groups. The results showed significant enrichment in several metabolic pathways, including phenylpropanoid biosynthesis (ko00940), nitrogen metabolism (ko00910), cutin, suberine, and wax biosynthesis (ko00073), photosynthesis-antenna proteins (ko00196), stilbenoid, diarylheptanoid, and gingerol biosynthesis (ko00945), flavonoid biosynthesis (ko00941), cyanoamino acid metabolism (ko00460), fatty acid elongation (ko00062), plant hormone signal transduction (ko04075), and alpha-linolenic acid metabolism (ko00592) (Fig. 2C and D; Tables S3 and S4).

Differentially accumulated proteins (DAPs) identification and functional annotation

To further explore the molecular mechanisms underlying the response of *R. sinensis* to varying salinity levels, we conducted a proteomic analysis under the same salt treatment and control conditions as the transcriptomic analysis. Proteins were characterized based on fold changes in their accumulation levels. Using DIA-based proteomic sequencing, we identified 6,273 peptides and 5,043 proteins (Fig. S5). Of these, 4,976 proteins were annotated in the NR database (98.67%), 5,043 proteins in the SubCell-Location database (100%), 4,604 proteins in the GO database (91.29%), 3,039 proteins in the KEGG database (60.26%), 4,608 proteins in the Pfam database (91.37%), and 4,815 proteins in the EggNOG

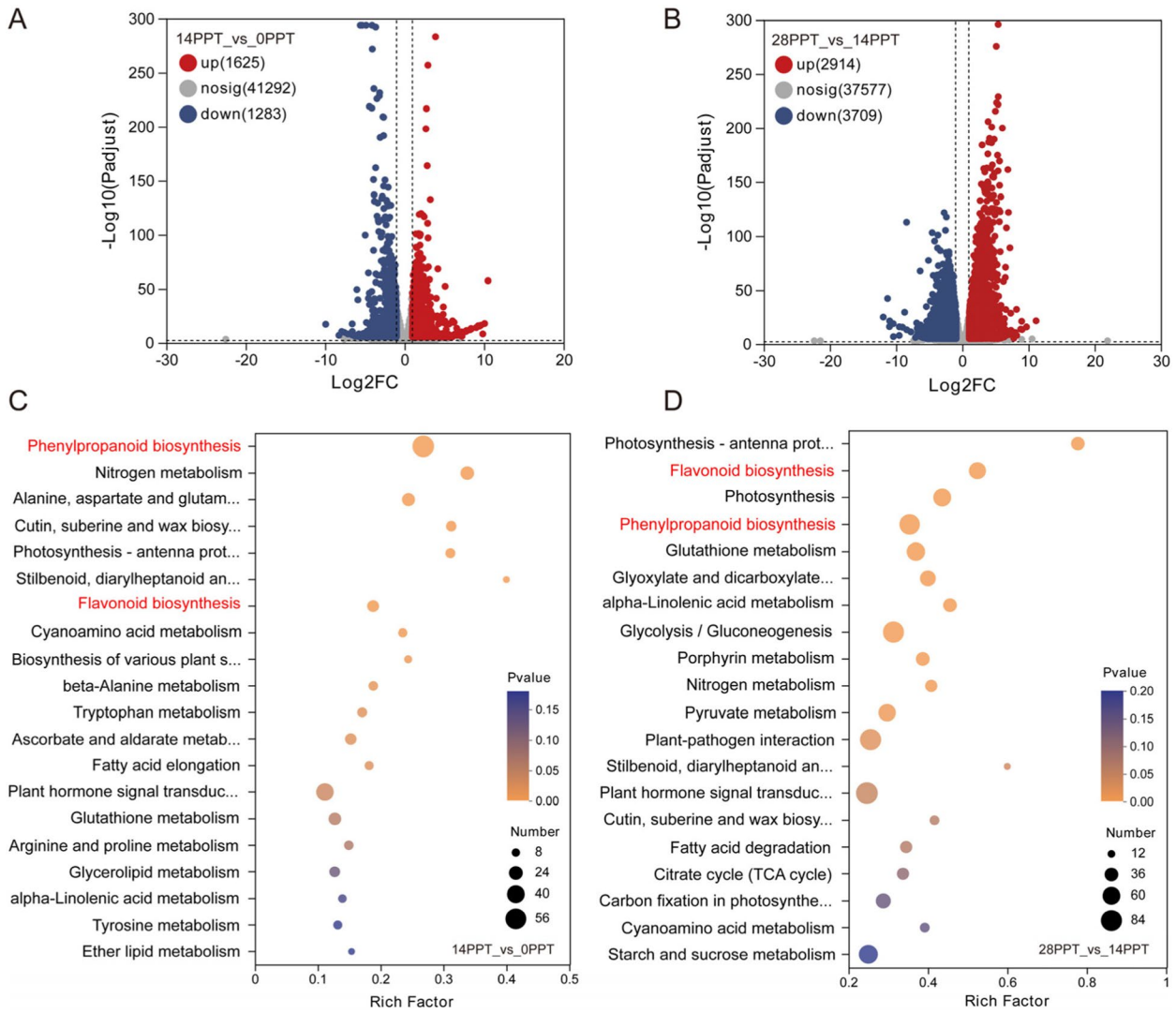

Fig. 2 Transcriptomic analysis of *Ruppia sinensis* under salt stress. (**A**) Number of DEGs in 14 PPT_vs_0 PPT. (**B**) Number of DEGs in 28 PPT_vs_14 PPT. (**C**, **D**) KEGG enrichment analysis of DEGs in 14 PPT_vs_0 PPT (**C**) and 28 PPT_vs_14 PPT (**D**)

database (95.48%) (Fig. S6). Pearson correlation coefficients and principal component analysis (PCA) were used to assess the correlation between all samples, and the results indicated good data reproducibility (Fig. S7).

In the 14 PPT_vs_0 PPT group, 1,139 DAPs were identified, with 445 proteins upregulated and 694 proteins downregulated. In the 28 PPT_vs_14 PPT group, 1,268 DAPs were identified, with 578 proteins upregulated and 690 proteins downregulated (Fig. 3A and B). Subcellular localization analysis showed that these DAPs were primarily distributed in the cytoplasm, chloroplast, nucleus, vacuole, mitochondria, and Golgi apparatus (Fig. 3C and D). Notably, over 50% of the DAPs were localized in the chloroplast and cytoplasm, indicating that the adaptation of *R. sinensis* to varying salinity levels may be closely associated with these two cellular structures. To further investigate the biological functions of these DAPs, we performed KEGG enrichment analysis. The results indicated significant enrichment in the phenylpropanoid biosynthesis pathway and its downstream flavonoid biosynthesis pathway in both comparison groups (Fig. 3E and F). This finding is consistent with the KEGG enrichment analysis of DEGs from the transcriptomic analysis (Fig. 2C and D), further emphasizing the critical role of the phenylpropanoid biosynthesis pathway in the response of *R. sinensis* to salinity fluctuations.

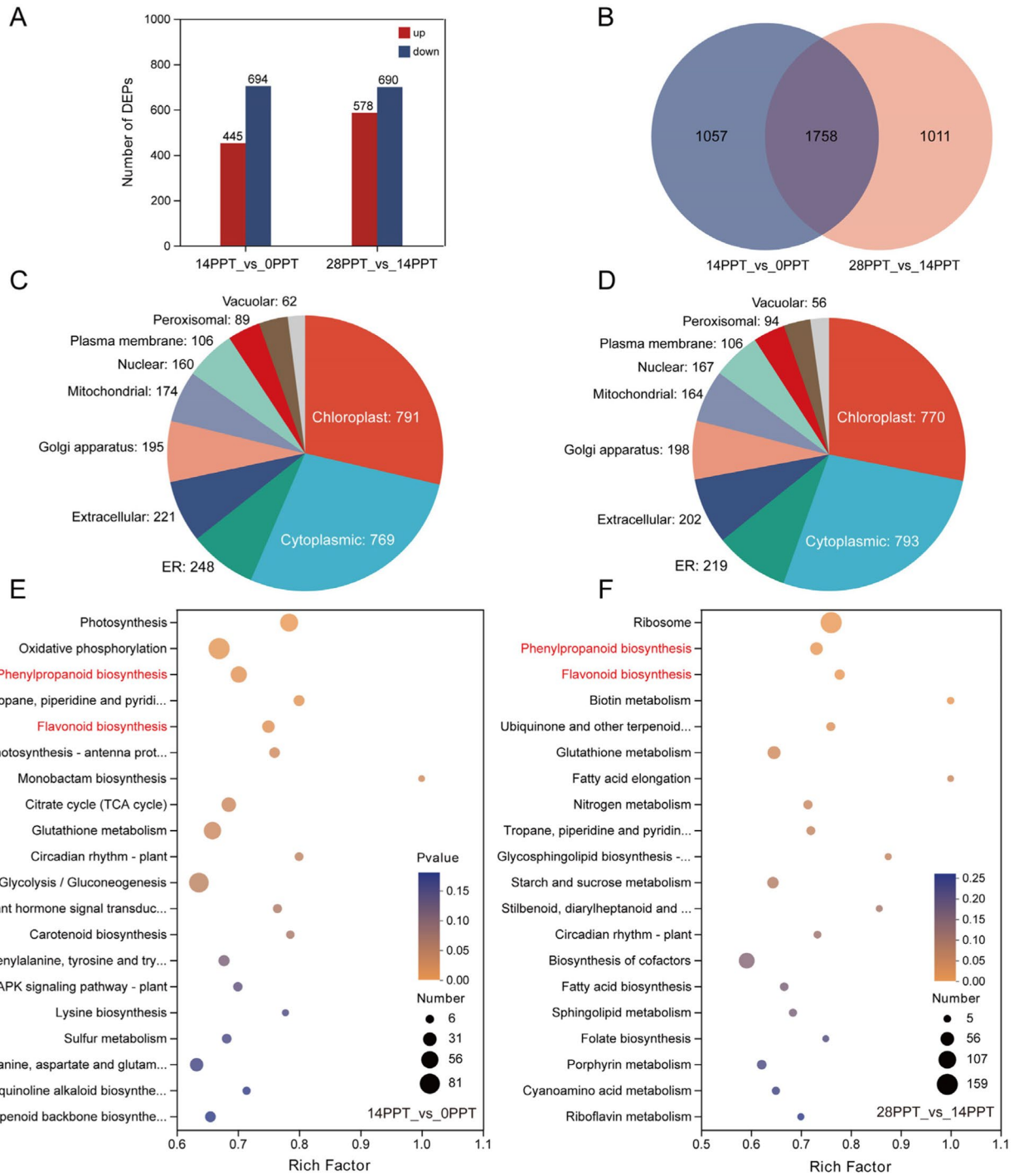

Fig. 3 Proteomic analysis of *Ruppia sinensis* under salt stress. (**A**) Number of DAPs in 14 PPT_vs_0 PPT and 28 PPT_vs_14 PPT. (**B**) Venn diagram of the DAPs in 14 PPT_vs_0 PPT and 28 PPT_vs_14 PPT. (**C**, **D**) Subcellular classification of DAPs in 14 PPT_vs_0 PPT (**C**) and 28 PPT_vs_14 PPT (**D**). (**E**, **F**) KEGG enrichment analysis of DAPs in 14 PPT_vs_0 PPT (**E**) and 28 PPT_vs_14 PPT (**F**)

Differentially accumulated metabolites (DAMs) identification and functional annotation

To better understand how varying water salinity affects the metabolites of *R. sinensis*, we conducted a comprehensive untargeted metabolomic analysis using UHPLC-MS/MS. A total of 875 metabolites were identified in positive ion mode, and 377 metabolites were identified in negative ion mode (Table S5). Among

these metabolites, primary metabolites accounted for 30%, with 371 identified, while secondary metabolites were more abundant, comprising 44% with 551 identified. Additionally, 320 metabolites (26%) were unclassified. In terms of annotation, 666 metabolites (53.19%) were successfully annotated to the KEGG database, 1,234 metabolites (95.56%) to the HMDB database, and 377 metabolites (30.11%) were mapped to specific KEGG pathways (Table S6). Metabolomic data from all samples across different treatment groups showed good reproducibility and reliability (Fig. S8).

In the 14 PPT_vs_0 PPT group, 225 metabolites were upregulated, 167 were downregulated, and 860 metabolites showed no significant changes (Fig. 4A). The upregulated metabolites were categorized into nine classes: steroids and derivatives (10.84%), lignans and derivatives (3.61%), indoles and derivatives (3.61%), alkaloids and derivatives (4.82%), phenolic acids and derivatives (7.23%), organic acids and derivatives (8.43%), flavonoids (8.43%), quinones (2.41%), and terpenoids (50.6%) (Fig. 4C). In the 28 PPT_vs_14 PPT group, the number of upregulated metabolites increased to 239, while the number of downregulated metabolites increased to 213, with 800 metabolites showing no significant changes (Fig. 4B). The upregulated metabolites were categorized into ten classes: alkaloids and derivatives (0.78%), stilbenes (3.10%), quinones (3.10%), lignans and derivatives (3.88%), organic acids and derivatives (5.43%), steroid acids and derivatives (6.20%), indoles and derivatives (10.85%), phenolic acids and derivatives (10.85%), coumarins and derivatives (12.40%), flavonoids (23.26%), and terpenoids (20.16%) (Fig. 4D). Consistent with the findings from transcriptomic and proteomic studies (Figs. 2 and 3), the phenylpropanoid biosynthesis pathway was significantly enriched among the DAMs (Fig. 4E and F). The proportion of flavonoids, which are secondary metabolites produced by the phenylpropanoid pathway, increased significantly from 8.43% (7 flavonoids) in the 14 PPT_vs_0 PPT group to 23.26% (30 flavonoids) in the 28 PPT_vs_14 PPT group, making them the largest category among the DAMs (Fig. 4C and D). This notable increase suggests that flavonoids may play a crucial role in the adaptation of *R. sinensis* to fluctuations in water salinity.

The expression of phenylpropanoid-related genes correlates with metabolites impacted by salt stress

By integrating transcriptomics and metabolomics for joint analysis, we can effectively mitigate issues such as noise and data loss that may occur when analyzing a single omics dataset. Transcriptomic analysis reveals the differential gene expression of *R. sinensis* in response to changes in water salinity, while metabolomics provides insights into changes in metabolites and their associated metabolic pathways. Through this integrated approach, we simultaneously annotated DEGs and DAMs to KEGG pathway maps, providing a deeper understanding of the relationship between genes and metabolites.

The results showed that in the 14 PPT_vs_0 PPT group, the enriched pathways included nitrogen metabolism (ko00910), starch and sucrose metabolism (ko00500), plant hormone signal transduction (ko04075), biosynthesis of cofactors (ko01240), phenylpropanoid biosynthesis (ko00940), vitamin B6 metabolism (ko00750), flavone and flavonol biosynthesis (ko00944), phenylalanine metabolism (ko00360), biosynthesis of various plant secondary metabolites (ko00999), and arachidonic acid metabolism (ko00590) (Fig. 5A). In the 28 PPT_vs_14 PPT group, the enriched pathways included plant-pathogen interaction (ko04626), phenylpropanoid biosynthesis (ko00940), glycolysis/gluconeogenesis (ko00010), plant hormone signal transduction (ko04075), biosynthesis of cofactors (ko01240), biosynthesis of unsaturated fatty acids (ko01040), phenylalanine metabolism (ko00360), tryptophan metabolism (ko00380), biosynthesis of various plant secondary metabolites (ko00999), and arachidonic acid metabolism (ko00590) (Fig. 5B).

In both comparison groups, the results of the integrated analysis were significantly enriched in the phenylpropanoid biosynthesis pathway (Fig. 5), consistent with the findings from the separate transcriptomic, proteomic, and metabolomic analyses. This suggests that the phenylpropanoid biosynthesis pathway likely plays a crucial role in the response of *R. sinensis* to fluctuations in water salinity. The integrated multi-omics analysis revealed that the phenylpropanoid pathway starts from phenylalanine and, through a series of enzymatic reactions—including phenylalanine ammonia-lyase (*PAL*), 4-coumarate-CoA ligase (*4CL*), and chalcone synthase (*CHS*)—ultimately produces various flavonoids and flavonols, such as eriodictyol, naringenin, luteolin, and quercetin (Fig. 6). In the 28 PPT_vs_14 PPT group, the transcript levels of the *PAL*, *CHS*, *F3H*, and *CYP73A* genes were significantly higher than in the 14 PPT_vs_0 PPT group, potentially promoting the production of more flavonoid compounds to help plants adapt to higher salinity environments. Additionally, to study the expression patterns of related genes, we randomly selected nine genes from this pathway for qRT-PCR analysis to verify the reliability of the transcriptomic data. The results showed that the gene expression levels determined by RNA sequencing were consistent with those measured by qRT-PCR (Fig. S9). In conclusion, the integration of multi-omics datasets indicates that the phenylpropanoid pathway is significantly enhanced under high salinity conditions and plays a pivotal role in the adaptation of *R. sinensis* to changes in water salinity.

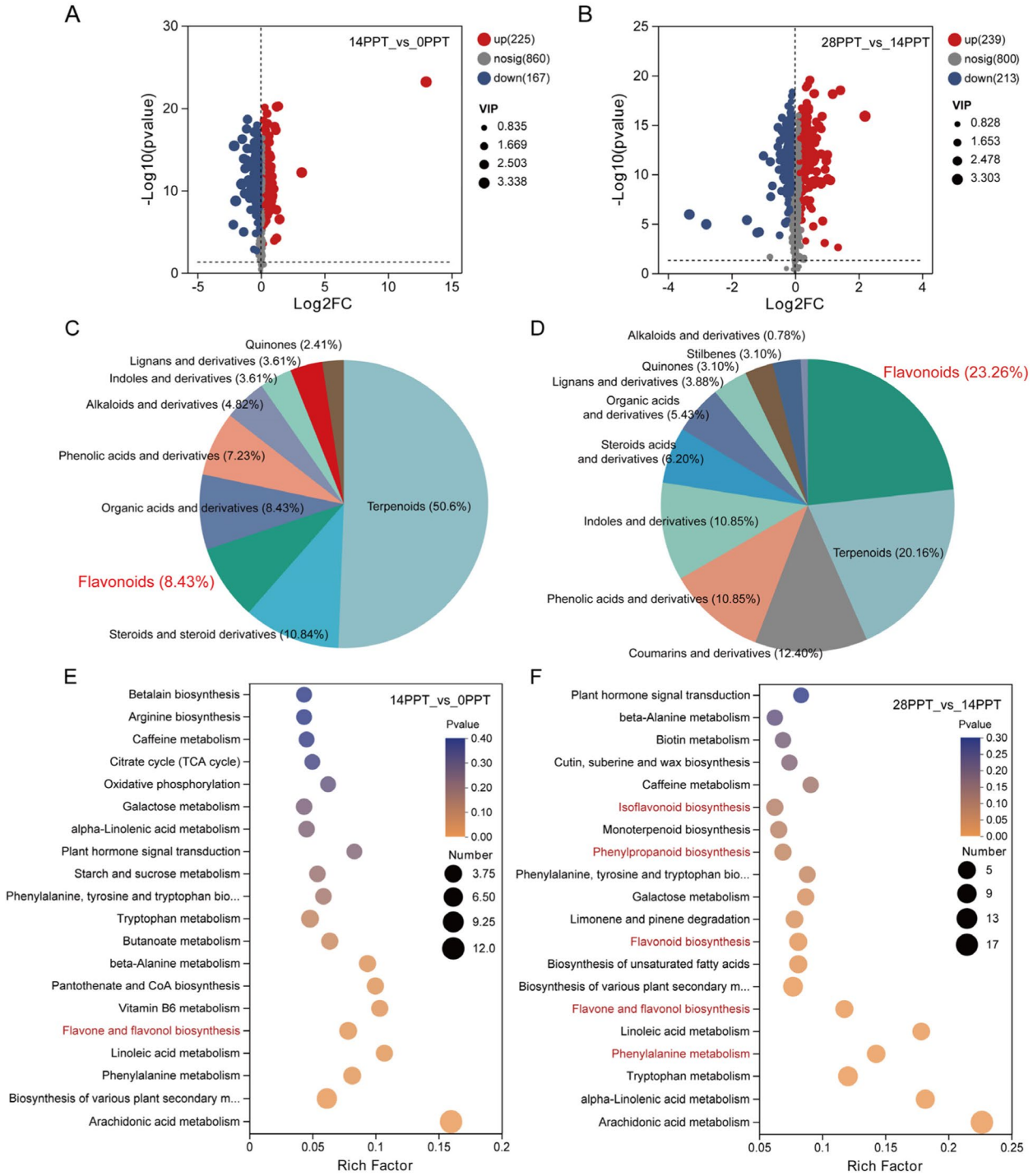

Fig. 4 Metabolomic analysis of *Ruppia sinensis* under salt stress. (**A**) Number of DAMs in 14 PPT_vs_0 PPT. (**B**) Number of DAMs in 28 PPT_vs_14 PPT. (**C**) Classification of DAMs in 14 PPT_vs_0 PPT under salt treatment. (**D**) Classification of DAMs in 28 PPT_vs_14 PPT under salt treatment. (**E**, **F**) KEGG enrichment analysis of DAMs in 14 PPT_vs_0 PPT (**E**) and 28 PPT_vs_14 PPT (**F**)

Discussion

Integrated multi-omics research has been widely used to study the genetic basis of plant adaptation to extreme environments [20, 29, 40, 54]. In this study, we conducted a comprehensive transcriptomic, proteomic, and metabolomic analysis of *R. sinensis* leaves under different salinity

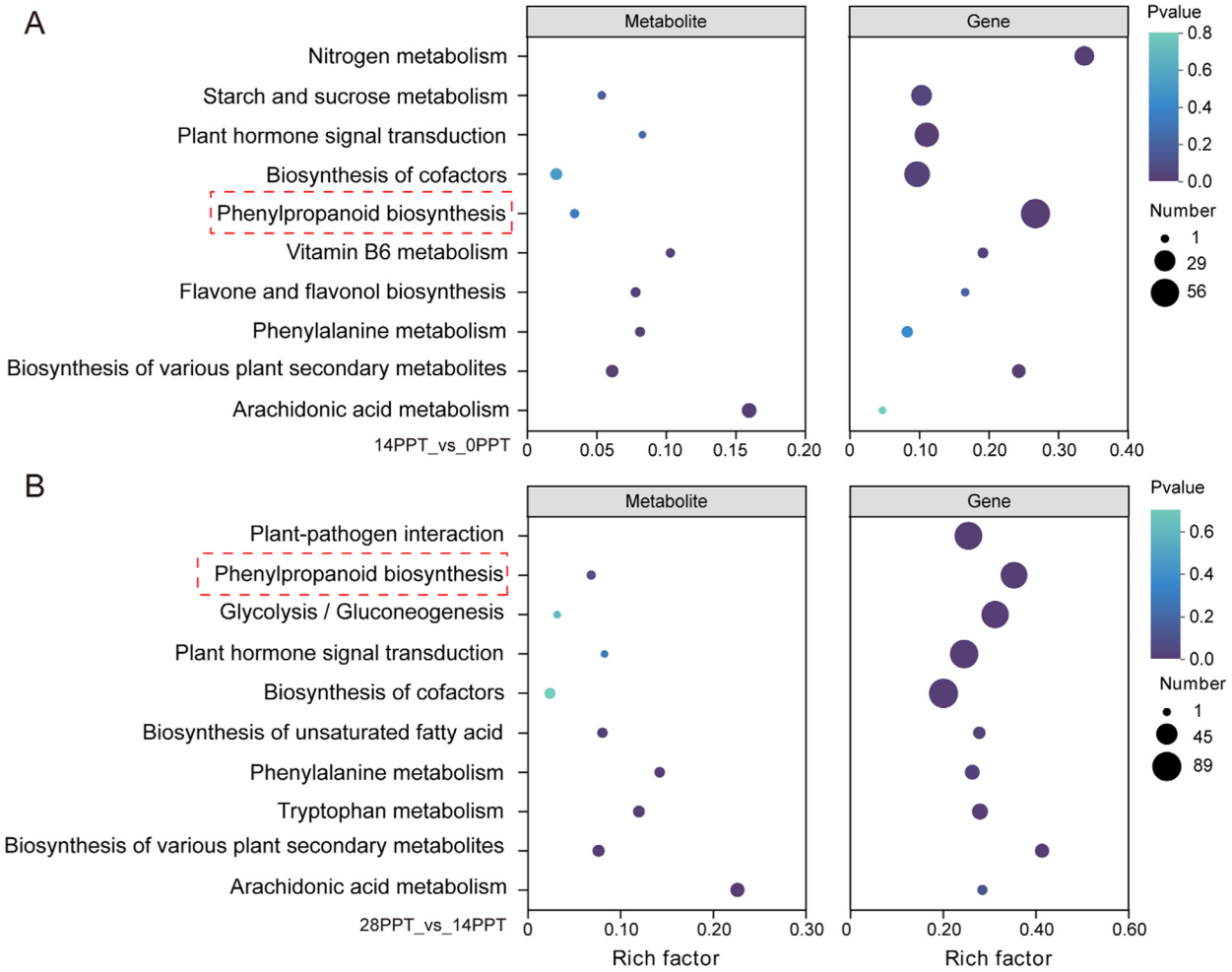

Fig. 5 Correlation analysis of transcriptome and metabolomics data. (**A**, **B**) KEGG enrichment analysis of combined transcriptome and metabolome data: (**A**) 14 PPT_vs_0 PPT, and (**B**) 28 PPT_vs_14 PPT. The x-axis shows the enrichment factor of the pathway in two omics, and the y-axis shows the name of the KEGG pathway; the color from red to green represents the significance of enrichment from high to low (indicated by the *P* value). The size of bubbles indicates the number of DEGs or DAMs; the larger the number, the larger the symbol. The shape of bubbles illustrates the various omics: the left side represents metabolomics, and the right side represents transcriptomics

conditions to explore the genetic mechanisms behind water salinity adaptation. Our results identified key regulatory defense pathways and metabolites involved in salt tolerance, which may enhance our understanding of the mechanisms underlying salinity adaptation in seagrasses.

Salt tolerance in plants contributes to their growth in adverse environments [4, 48, 67]. When subjected to salt stress, plants generate harmful reactive oxygen species (ROS) [47]. Excessive ROS can inhibit plant growth and even lead to cell death. To eliminate these ROS, plants employ both enzymatic and non-enzymatic antioxidants as a defense [17, 22, 24]. Enhancing the activity of antioxidant enzymes and producing non-enzymatic antioxidants are key ways in which plants mitigate ROS damage [1]. In this study, we found that several physiological indicators, such as CAT, POD, SOD, MDA, and SP, increased with rising salinity levels. This indicated that the plant activated an antioxidant defense system by increasing the activities of CAT, POD, and SOD to eliminate excess ROS and mitigate oxidative stress. Meanwhile, the elevated levels of MDA indicated oxidative damage to cell membranes, while the increase in soluble proteins helped regulate osmotic pressure, protecting cell structure and function [21]. By upregulating antioxidant enzyme activities, the plant maintained lower ROS levels, protecting the photosynthetic machinery and sustaining growth under salt stress [74]. Additionally, over 50% of the differentially expressed proteins (DAPs) were localized in the chloroplast and cytoplasm. The decline in chlorophyll content with increasing salinity suggests that high

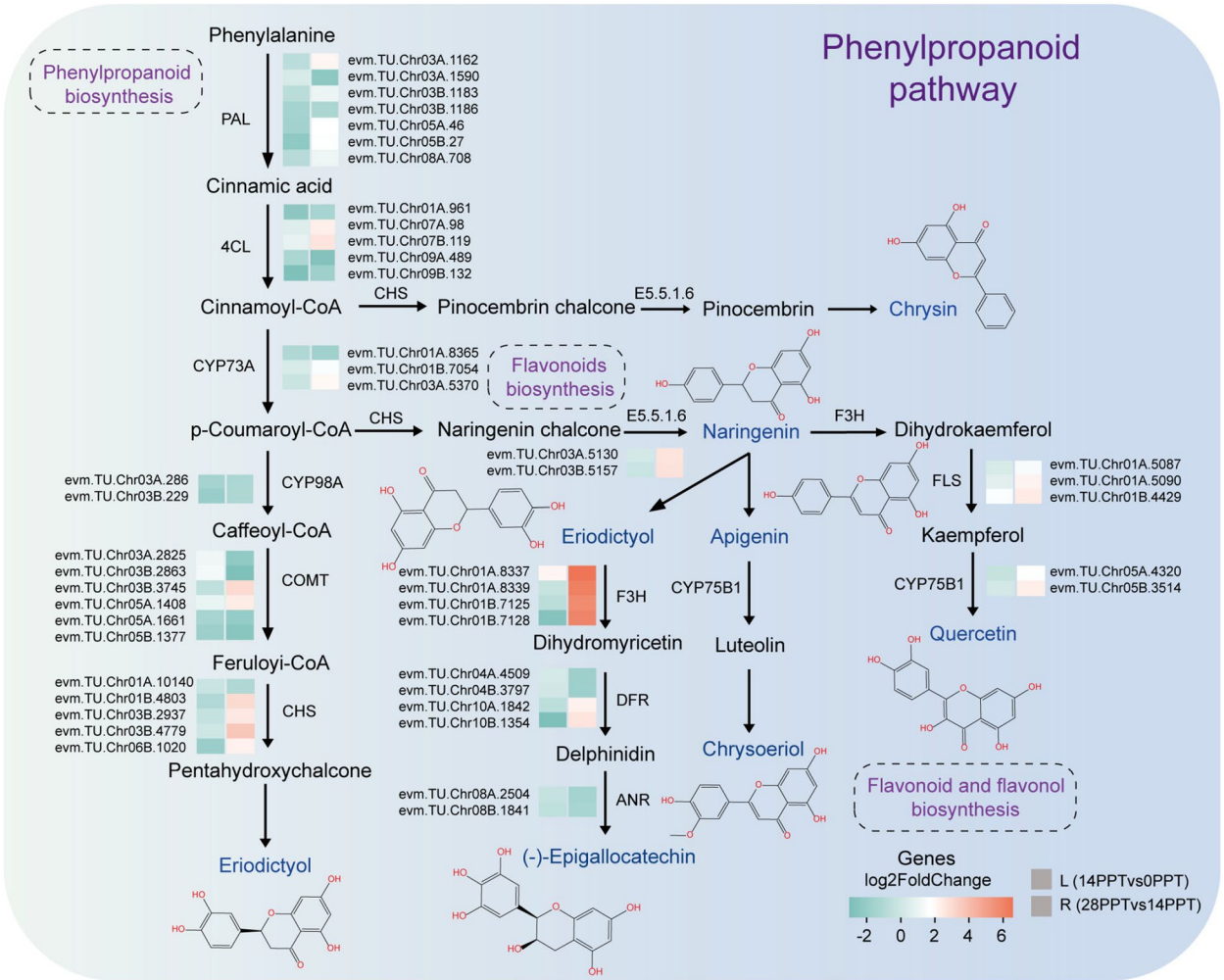

Fig. 6 Regulation of key metabolic pathway at different salinity, with colors indicating the log2Fold Change values (14 PPT_vs_0 PPT/28 PPT_vs_14 PPT). Each box represents the expression differences of related genes under varying salt treatments, with red denoting upregulated and green indicating downregulated genes. Metabolites marked in blue font represent those detected by metabolomic sequencing in this study

salinity disrupts chloroplast structure and function, leading to reduced photosynthetic efficiency and negatively impacting plant growth and survival. This phenomenon has also been observed in terrestrial plants [12, 44, 57]. These findings suggest that antioxidant enzymes play a crucial role in ROS scavenging in *R. sinensis* under salt stress conditions.

In addition to the enzymatic antioxidant system, non-enzymatic antioxidants also play a vital role in the response of *R. sinensis* to salt stress. Flavonoids, a group of secondary metabolites, are widely distributed in plants [64]; Samanta et al., [58]; Panche et al., [42, 49]. They perform various biochemical and molecular functions, such as plant defense, signaling, and antioxidant activities [3]. Flavonoids help plants adapt and survive under salt stress through multiple mechanisms, including antioxidant activity, ion balance regulation, signal transduction modulation, and growth and development regulation. As non-enzymatic antioxidants, flavonoids accumulate in various plant tissues and aid in free radicals scavenging, thereby enhancing salt tolerance [37, 55]. In this study, transcriptomic and proteomic analyses revealed the activation of genes and proteins in the phenylpropanoid pathway of *R. sinensis* under different water salinity conditions. This process led to the accumulation of various flavonoids, which enhanced the ability of the plant to eliminate ROS. Metabolomic analysis revealed significant changes in the abundance of terpenoid and flavonoid metabolites in the 14 PPT_vs_0 PPT, and the 28 PPT_vs_14 PPT groups (Fig. 4A and B). As products of the phenylpropanoid biosynthesis pathway, flavonoids represented a significant proportion of the differential metabolites. When comparing flavonoid metabolites within the phenylpropanoid pathway to identify those associated

with salt tolerance, we observed an increase from 8.43% (7 flavonoids) in the 14 PPT_vs_0 PPT to 23.26% (30 flavonoids) in the 28 PPT_vs_14 PPT, making flavonoids the most prominent category among the differential metabolites (Fig. 4C and D). These findings suggest that flavonoids, as non-enzymatic antioxidants, complement the enzymatic antioxidant system in mitigating oxidative stress under salinity fluctuations.

Among these flavonoids, quercetin is a well-known compound with potent antioxidant properties due to its ability to scavenge ROS and chelate metal ions involved in ROS generation [33, 53]. Under salt stress, accumulation of quercetin in plants has been shown to mitigate oxidative damage by neutralizing free radicals, thereby protecting cellular components such as lipids, proteins, and DNA from oxidative stress [36]. In addition, quercetin regulates the activity of antioxidant enzymes, enhancing their ability to counteract oxidative damage [71]. This is consistent with our findings that antioxidant enzymes (CAT, POD, and SOD) exhibited significantly increased activities under high salinity (Fig. 1A-C), while quercetin biosynthesis genes in the phenylpropanoid pathway were significantly upregulated (Fig. 6). This indicates that quercetin plays an important role in scavenging ROS and maintaining cellular redox balance, thereby enhancing the antioxidant defense capacity of *R. sinensis* under high salinity conditions. These results suggest that, similar to terrestrial plants, *R. sinensis* adapts to high salinity in aquatic environments by producing more flavonoids, and the phenylpropanoid pathway likely plays a key role in the plant's response to fluctuating salinity levels.

Supplementary Information

The online version contains supplementary material available at https://doi.org/10.1186/s12870-025-06189-3.

Additional file 1.

Additional file 2.

Acknowledgements
This study was supported by the Special Project of Basic Work of Science and Technology, Ministry of Science and Technology, China (No. 2013FY112300).

Authors' contributions
X.X designed the research; X.X. and Y.Z. carried out the field collections; Y.Z. carried out the experiments and performed the data analysis; Y.Z. drafted the manuscript. X.X. revised the manuscript. All authors approved the final manuscript.

Funding
This study was supported by the Special Project of Basic Work of Science and Technology, Ministry of Science and Technology, China (No. 2013FY112300).

Data availability
All raw sequencing data from this study have been deposited in the Genome Sequence Archive in National Genomics Data Center under the accession number: CRA018784 (https://ngdc.cncb.ac.cn/gsa/browse/CRA018784).

Declarations

Ethics approval and consent to participate
The *Ruppia sinensis* seed materials used in this study were collected with the approval of local regulatory authorities. All methods were carried out in compliance with local and national regulations.

Consent for publication
Not applicable.

Competing interests
The authors declare no competing interests.

Received: 4 November 2024 Accepted: 31 January 2025
Published online: 10 February 2025

References

1. Ahmad P, Jaleel CA, Azooz MM, Nabi G. Generation of ROS and non-enzymatic antioxidants during abiotic stress in plants. Bot Res Int. 2009;2:11–20.
2. Anders S, Huber W. (2012). Differential expression of RNA-Seq data at the gene level–the DESeq package. Heidelberg, Germany: Europ Molecular Biol Laborat. (EMBL), 10, f1000research.
3. Barreca D, Gattuso G, Bellocco E, Calderaro A, Trombetta D, Smeriglio A, Laganà G, Daglia M, Meneghini S, Nabavi SM. Flavanones: Citrus phytochemical with health-promoting properties. BioFactors. 2017;43:495–506.
4. Bartels D, Sunkar R. Drought and salt tolerance in plants. CRC Crit Rev Plant Sci. 2005;24(1):23–58.
5. Bateman A, Coin L, Durbin R, Finn RD, Hollich V, Griffiths-Jones S, Eddy SR. The pfam protein families database. Nucleic Acids Res. 2004;32(suppl1):D138–41.
6. Bekker-Jensen DB, Bernhardt OM, Hogrebe A, Martinez-Val A, Verbeke L, Gandhi T, Olsen JV. Rapid and site-specific deep phosphoproteome profiling by data-independent acquisition without the need for spectral libraries. Nat Commun. 2020;11(1):787.
7. Boeckmann B, Bairoch A, Apweiler R, Blatter MC, Estreicher A, Gasteiger E, Schneider M. The SWISS-PROT protein knowledgebase and its supplement TrEMBL in 2003. Nucleic Acids Res. 2003;31(1):365–70.
8. Boratyn GM, Camacho C, Cooper PS, Coulouris G, Fong A, Ma N, Zaretskaya I. BLAST: a more efficient report with usability improvements. Nucleic Acids Res. 2013;41(W1):W29–33.
9. Borum J, Duarte CM, Krause-Jensen D, Greve TM. 2004. European seagrasses: An introduction to monitoring and management. Copenhagen: Monitoring & Managing of European Seagrass Ecosystems (M&MS) project; 2004.
10. Brock MA. Biology of the salinity tolerant genus Ruppia L. in saline lakes in South Australia II. Population ecology and reproductive biology. Aquat Bot. 1982;13:249–68.
11. Bradford MM. A rapid and sensitive method for the quantitation of microgram quantities of protein utilizing the principle of protein-dye binding. Anal Biochem. 1976;72(1–2):248–54.
12. Cao H, Han Y, Cheng Z, Lv Q, Pompelli MF, Pereira JD, Araújo WL. Long exposure to salt stress in Jatropha curcas leads to stronger damage to the chloroplast ultrastructure and its functionality than the stomatal function. Forests. 2023;14(9):1868.
13. Carillo P, Annunziata MG, Pontecorvo G, Fuggi A, Woodrow P. Salinity stress and salt tolerance. Abiotic Stress plants-mechanisms Adaptations. 2011;1:21–38.
14. Chai L, Yang L, Zhang Y, Zhou Y, Wang F, Wu Z. Antagonism or synergism? Responses of Hydrocharis Dubia (bl.) Backer to linear alkylbenzene sulfonate, naphthalene and their joint exposure. Ecotoxicol Environ Saf. 2020;200:110747.
15. Chen S, Zhou Y, Chen Y, Gu J. Fastp: an ultra-fast all-in-one FASTQ preprocessor. Bioinformatics. 2018;34(17):i884–90.
16. Dabravolski SA, Isayenkov SV. The regulation of plant cell wall organisation under salt stress. Front Plant Sci. 2023;14:1118313.

17. Das K, Roychoudhury A. Reactive oxygen species (ROS) and response of antioxidants as ROS-scavengers during environmental stress in plants. Front Environ Sci. 2014;2:53.
18. Duarte CM, Marbà N, Gacia E, Fourqurean JW, Beggins J, Barrón C, Apostolaki ET. Seagrass community metabolism: assessing the carbon sink capacity of seagrass meadows. Glob Biogeochem Cycles. 2010;24:2010GB003793.
19. Feng W, Lindner H, Robbins NE, Dinneny JR. Growing out of stress: the role of cell-and organ-scale growth control in plant water-stress responses. Plant Cell. 2016;28(8):1769–82.
20. Feng X, Xu S, Li J, Yang Y, Chen Q, Lyu H, Shi S. Molecular adaptation to salinity fluctuation in tropical intertidal environments of a mangrove tree Sonneratia alba. BMC Plant Biol. 2020;20:1–14.
21. Garcia-Caparros P, De Filippis L, Gul A, Hasanuzzaman M, Ozturk M, Altay V, Lao MT. Oxidative stress and antioxidant metabolism under adverse environmental conditions: a review. Bot Rev. 2021;87:421–66.
22. Gao Y, Long R, Kang J, Wang Z, Zhang T, Sun H, Li X, Yang Q. Comparative proteomic analysis reveals that antioxidant system and soluble sugar metabolism contribute to salt tolerance in alfalfa (Medicago sativa L.) leaves. J Proteome Res. 2018;18:191–203.
23. Geddesa MC, Deckkera PD, Williamsa WD, Morton DW, Topping M. On the chemistry and biota of some saline lakes in Western Australia. In Williams WD, editor. Salt Lakes. Developments in Hydrobiology, vol 5. Dordrecht: Springer; 1981. p. 201–22.
24. Gill SS, Tuteja N. Reactive oxygen species and antioxidant machinery in abiotic stress tolerance in crop plants. Plant Physiol Biochem. 2010;48(12):909–30.
25. Gu R, Zhou Y, Song X, Xu S, Zhang X, Lin H, Zhu S. Effects of temperature and salinity on Ruppia sinensis seed germination, seedling establishment, and seedling growth. Mar Pollut Bull. 2018;134:177–85.
26. Gu R, Song X, Zhou Y, Xu S, Xu S, Yue S, Zhang X. Relationships between Annual and Perennial Seagrass (Ruppia Sinensis) populations and their sediment geochemical characteristics in the Yellow River Delta. Front Plant Sci. 2021;12:634199.
27. Hao S, Wang Y, Yan Y, Liu Y, Wang J, Chen S. A review on plant responses to salt stress and their mechanisms of salt resistance. Horticulturae. 2021;7(6):132.
28. Hasanuzzaman M, Raihan MRH, Masud AAC, Rahman K, Nowroz F, Rahman M, Fujita M. Regulation of reactive oxygen species and antioxidant defense in plants under salinity. Int J Mol Sci. 2021;22(17):9326.
29. Han T, Mi Z, Chen Z, Zhao J, Zhang H, Lv Y, Ge S. Multi-omics analysis reveals the influence of tetracycline on the growth of ryegrass root. J Hazard Mater. 2022;435:129019.
30. Hossain MS, Dietz KJ. Tuning of redox regulatory mechanisms, reactive oxygen species and redox homeostasis under salinity stress. Front Plant Sci. 2016;7:548.
31. Holmes GD, Hall NE, Gendall AR, Boon PI, James EA. Using transcriptomics to identify differential gene expression in response to salinity among Australian Phragmites australis clones. Front Plant Sci. 2016;7:432.
32. Huerta-Cepas J, Szklarczyk D, Heller D, Hernández-Plaza A, Forslund SK, Cook H, Bork P. eggNOG 5.0: a hierarchical, functionally and phylogenetically annotated orthology resource based on 5090 organisms and 2502 viruses. Nucleic Acids Res. 2019;47(D1):D309–14.
33. Jomova K, Alomar SY, Alwasel SH, Nepovimova E, Kuca K, Valko M. Several lines of antioxidant defense against oxidative stress: antioxidant enzymes, nanomaterials with multiple enzyme-mimicking activities, and low-molecular-weight antioxidants. Arch Toxicol. 2024;98(5):1323–67.
34. Kanehisa M, Araki M, Goto S, Hattori M, Hirakawa M, Itoh M, Yamanishi Y. KEGG for linking genomes to life and the environment. Nucleic Acids Res. 2007;36(suppl1):D480–4.
35. Kerchev PI, Van Breusegem F. Improving oxidative stress resilience in plants. Plant J. 2022;109(2):359–72.
36. Kesawat MS, Satheesh N, Kherawat BS, Kumar A, Kim HU, Chung SM, Kumar M. Regulation of reactive oxygen species during salt stress in plants and their crosstalk with other signaling molecules—current perspectives and future directions. Plants. 2023;12(4):864.
37. Kiani R, Arzani A, Mirmohammady Maibody SAM. Polyphenols, flavonoids, and antioxidant activity involved in salt tolerance in wheat, Aegilops cylindrica and their amphidiploids. Front Plant Sci. 2021;12:646221.
38. Kim D, Langmead B, Salzberg SL. HISAT: a fast spliced aligner with low memory requirements. Nat Methods. 2015;12(4):357–60.
39. Kumar S, Abedin MM, Singh AK, Das S. Role of phenolic compounds in plant-defensive mechanisms. Plant Phenolics Sustainable Agriculture: Volume. 2020;1:517–32.
40. Li Z, Xu C, Wang J. Integrated physiological, transcriptomic and proteomic analyses revealed molecular mechanism for salt resistance in Solidago canadensis L. Environ Exp Bot. 2020;179:104211.
41. Lichtenthaler HK, Wellburn AR. Determinations of total carotenoids and chlorophylls a and b of leaf extracts in different solvent. Biochem Soc T. 1983;11(5):591–2.
42. Liu X, Cheng X, Cao J, Zhu W, Wan X, Liu L. GOLDEN 2-LIKE transcription factors regulate chlorophyll biosynthesis and flavonoid accumulation in response to UV-B in tea plants. Hortic Plant J. 2023;9:1055–66.
43. Masmoudi S, Tastard E, Guermazi W, Caruso A, Morant-Manceau A, Ayadi H. Salinity gradient and nutrients as major structuring factors of the phytoplankton communities in salt marshes. Aquat Ecol. 2015;49:1–19.
44. Manaa A, Goussi R, Derbali W, Cantamessa S, Abdelly C, Barbato R. Salinity tolerance of quinoa (Chenopodium quinoa Willd) as assessed by chloroplast ultrastructure and photosynthetic performance. Environ Exp Bot. 2019;162:103–14.
45. Mishra N, Jiang C, Chen L, Paul A, Chatterjee A, Shen G. Achieving abiotic stress tolerance in plants through antioxidative defense mechanisms. Front Plant Sci. 2023;14:1110622.
46. Munns R. Comparative physiology of salt and water stress. Plant Cell Environ. 2002;25:239–50.
47. Nishiyama Y. Oxidative stress inhibits the repair of photodamage to the photosynthetic machinery. EMBO J. 2001;20:5587–94.
48. Parida AK, Das AB. Salt tolerance and salinity effects on plants: a review. Ecotoxicol Environ Saf. 2005;60(3):324–49.
49. Panche AN, Diwan AD, Chandra SR. (2016). Flavonoids: an overview. J Nutritional Sci, 5, e47.
50. Pang Z, Chong J, Zhou G, de Lima Morais DA, Chang L, Barrette M, Xia J. MetaboAnalyst 5.0: narrowing the gap between raw spectra and functional insights. Nucleic Acids Res. 2021;49(W1):W388–96.
51. Pratyusha S. Phenolic compounds in the plant development and defense: an overview. In: Hasanuzzaman M, Nahar K, editors. Plant stress physiology-perspectives in agriculture. London: IntechOpen; 2022. p. 125–40.
52. Putri GH, Anders S, Pyl PT, Pimanda JE, Zanini F. Analysing high-throughput sequencing data in Python with HTSeq 2.0. Bioinformatics. 2022;38(10):2943–5.
53. Qi W, Qi W, Xiong D, Long M. Quercetin: its antioxidant mechanism, antibacterial properties and potential application in prevention and control of toxipathy. Molecules. 2022;27(19):6545.
54. Ren H, Yang W, Jing W, Shahid MO, Liu Y, Qiu X, Zhou X. Multi-omics analysis reveals key regulatory defense pathways and genes involved in salt tolerance of rose plants. Hortic Res. 2024;11(5):uhae068.
55. Rezayian M, Niknam V, Ebrahimzadeh H. Oxidative damage and antioxidative system in algae. Toxicol Rep. 2019;6:1309–13.
56. Sahoo JP, Behera L, Sharma SS, Praveena J, Nayak SK, Samal KC. Omics studies and systems biology perspective towards abiotic stress response in plants. Am J Plant Sci. 2020;11:2172–94.
57. Salama S, Trivedi S, Busheva M, Arafa AA, Garab G, Erdei L. Effects of NaCl salinity on growth, cation accumulation, chloroplast structure and function in wheat cultivars differing in salt tolerance. J Plant Physiol. 1994;144(2):241–7.
58. Samanta A, Das G, Das SK. Roles of flavonoids in plants. Int J Pharm Sci Tech. 2011;6(1):12–35.
59. Shabala SN, Lew RR. Turgor regulation in osmotically stressed arabidopsis epidermal root cells. Direct support for the role of inorganic ion uptake as revealed by concurrent flux and cell turgor measurements. Plant Physiol. 2002;129:290–9.
60. Shomali A, Das S, Arif N, Sarraf M, Zahra N, Yadav V, Hasanuzzaman M. Diverse physiological roles of flavonoids in plant environmental stress responses and tolerance. Plants. 2022;11(22):3158.
61. Swift ML. GraphPad prism, data analysis, and scientific graphing. J Chem Inf Comput Sci. 1997;37(2):411–2.
62. Soares C, Carvalho ME, Azevedo RA, Fidalgo F. Plants facing oxidative challenges—A little help from the antioxidant networks. Environ Exp Bot. 2019;161:4–25.

63. Sud M, Fahy E, Cotter D, Brown A, Dennis EA, Glass CK, Merrill AH Jr, Murphy RC, Raetz CR, Russell DW, Subramaniam S. LMSD: LIPID MAPS structure database. Nucleic Acids Res. 2007;35(suppl1):D527–32.
64. Treutter D. Significance of flavonoids in plant resistance: a review. Environ Chem Lett. 2006;4(3):147–57.
65. Touchette BW. Seagrass-salinity interactions: physiological mechanisms used by submersed marine angiosperms for a life at sea. J Exp Mar Biol Ecol. 2007;350:194–215.
66. Touchette BW, Smith GA, Rhodes KL, Poole M. Tolerance and avoidance: two contrasting physiological responses to salt stress in mature marsh halophytes Juncus roemerianus Scheele and Spartina alterniflora Loisel. J Exp Mar Biol Ecol. 2009;380(1–2):106–12.
67. Tuteja N. Mechanisms of high salinity tolerance in plants. Methods Enzymol. 2007;428:419–38.
68. Vogt T. Phenylpropanoid biosynthesis. Mol Plant. 2010;3(1):2–20.
69. Wishart DS, Tzur D, Knox C, Eisner R, Guo AC, Young N, Querengesser L. HMDB: the human metabolome database. Nucleic Acids Res. 2007;35(suppl1):D521–6.
70. Xu C, Li Z, Wang J. Linking heat and adaptive responses across temporal proteotranscriptome and physiological traits of Solidago canadensis. Environ Exp Bot. 2020;175:104035.
71. Xu D, Hu MJ, Wang YQ, Cui YL. Antioxidant activities of quercetin and its complexes for medicinal application. Molecules. 2019;24(6):1123.
72. Yadav V, Wang Z, Wei C, Amo A, Ahmed B, Yang X, Zhang X. Phenylpropanoid pathway engineering: an emerging approach towards plant defense. Pathogens. 2020;9(4):312.
73. Yu G, Wang LG, Han Y, He QY. clusterProfiler: an R package for comparing biological themes among gene clusters. OMICS. 2012;16(5):284–7.
74. Zahra N, Al Hinai MS, Hafeez MB, Rehman A, Wahid A, Siddique KH, Farooq M. Regulation of photosynthesis under salt stress and associated tolerance mechanisms. Plant Physiol Biochem. 2022;178:55–69.

Publisher's Note